Astronomy & Astrophysics manuscript no. var73dra2 February 2, 2008
(DOI: will be inserted by hand later)

arXiv:astro-ph/0302538v1 26 Feb 2003

In-the-Gap SU UMa-Type Dwarf Nova, Var73 Dra with a Supercycle of about 60 Days

Daisaku Nogami[1], Makoto Uemura[2], Ryoko Ishioka[2], Taichi Kato[2], Ken'ichi Torii[3], Donn R. Starkey[4], Kenji Tanabe[5], Tonny Vanmunster[6], Elena P. Pavlenko[7,8], Vitalij P. Goranskij[9], Elena A. Barsukova[10], Oksana Antoniuk[7,8], Brian Martin[11], Lewis M. Cook[12], Gianluca Masi[13], and Franco Mallia[14]

[1] Hida Observatory, Kyoto University, Kamitakara, Gifu 506-1314, Japan
[2] Department of Astronomy, Kyoto University, Kyoto 606-8502, Japan
[3] Cosmic Radiation Laboratory, Institute of Physical and Chemical Research (RIKEN), 2-1, Wako, Saitama 351-0198, Japan
[4] DeKalb Observatory, 2507 County Road 60, Auburn, Auburn, Indiana 46706, USA
[5] Department of Biosphere-Geosphere Systems, Faculty of Informatics, Okayama University of Science, 1-1 Ridaicho, Okayama 700-0005, Japan
[6] Center for Backyard Astrophysics (Belgium), Walhostraat 1A, B-3401 Landen, Belgium
[7] Crimean Astrophysical Observatory, Nauchny, 98409 Crimea, Ukraine
[8] Isac Newton Institute of Chile, Crimean Branch, Ukraine
[9] Sternberg Astronomical Institute, 119899, Moscow, Russia
[10] Special Astrophysical Observatory, Russian Academy of Sciences, Nizhnij Arkhyz, Karachaevo-Cherkesia, Russia
[11] King's University College, Department of Physics, 9125 50th Street, Edmonton, AB T5H 2M1, Canada
[12] Center for Backyard Astrophysics (Concord), 1730 Helix Court, Concord, CA 94518, USA
[13] Physics Department, University of Rome "Tor Vergata" Via della Ricerca Scientifica, 1 00133 Rome, Italy
[14] Campo Catino Astronomical Observatory 03025 Guarcino, Italy

Received ; accepted

Abstract.
An intensive photometric-observation campaign of the recently discovered SU UMa-type dwarf nova, Var73 Dra was conducted from 2002 August to 2003 February. We caught three superoutbursts in 2002 October, December and 2003 February. The recurrence cycle of the superoutburst (supercycle) is indicated to be ~60 d, the shortest among the values known so far in SU UMa stars and close to those of ER UMa stars. The superhump periods measured during the first two superoutbursts were 0.104885(93) d, and 0.10623(16) d, respectively. A 0.10424(3)-d periodicity was detected in quiescence. The change rate of the superhump period during the second superoutburst was 1.7×10^{-3}, which is an order of magnitude larger than the largest value ever known. Outburst activity has changed from a phase of frequent normal outbursts and infrequent superoutbursts in 2001 to a phase of infrequent normal outbursts and frequent superoutbursts in 2002. Our observations are negative to an idea that this star is an related object to ER UMa stars in terms of the duty cycle of the superoutburst and the recurrence cycle of the normal outburst. However, to trace the superhump evolution throughout a superoutburst, and from quiescence more effectively, may give a fruitful result on this matter.

Key words. Accretion, accretion disks – novae, cataclysmic variables — Stars: dwarf novae — Stars: individual (Var73 Dra)

1. Introduction

Dwarf novae are a class of cataclysmic variables stars (CVs), which show various types of variability originating in the accretion disk around the white dwarf (for a review, Warner 1995). Dwarf novae are further classified into three basic types of SS Cyg-type dwarf novae showing normal outbursts, Z Cam-type dwarf novae showing normal outbursts and standstills, and SU UMa-type dwarf novae showing superoutbursts as well as normal outbursts. The difference of photometric behavior in these kinds of stars including nova-like variable stars is essentially explained by the thermal-tidal disk instability scheme (for a review, e.g. Osaki 1996). Superhumps are oscillations with an amplitude of 0.1–0.5 mag and a period 1–5 % longer than the orbital period ($P_{\rm orb}$) observed only during long, bright (super)outbursts. The superhump is considered to be a beat phenomenon of the orbital motion of the secondary star and the precession of the tidally distorted eccentric disk (Whitehurst, 1988). The eccentricity in such disks plays a key role to keep

Send offprint requests to: D. Nogami (nogami@kwasan.kyoto-u.ac.jp)

the accretion disk in the hot state to make a normal outburst evolve into a superoutburst (Osaki, 1989).

Non-magnetic CVs have been suggested to have a bi-modal $P_{\rm orb}$ distribution (Robinson, 1983), while the gap between ∼2 h and ∼3 h seems to be filled in the case of magnetic systems (Webbink & Wickramasinghe, 2002). This period gap is explained in the standard theory of the CV evolution as follows: 1) the magnetic braking, which is the mechanism of angular momentum loss, suddenly dies down when the secondary star become fully convective around $P_{\rm orb}$∼3 h, 2) the secondary shrinks into the thermal equilibrium state and the mass transfer stops, 3) the angular-momentum loss is continued by a greatly reduced rate by the gravitational wave radiation, and 4) the secondary fills again its Roche-lobe around $P_{\rm orb}$∼2 h and the CV activity restarts (for a review, King 1988). Although most of the SU UMa-type dwarf novae are distributed below the period gap, some systems are above (TU Men: Mennickent 1995) and in (e.g. NY Ser: Nogami et al. 1998b) the period gap.

The evolution scenario predicts that CVs evolve for the shorter $P_{\rm orb}$ region with the mass transfer rate ($\dot{M}$) reduced, but the orbital period begins to increase after the secondary is degenerated (Paczyński, 1971; Kolb & Baraffe, 1999). Most SU UMa stars are believed to be on this standard path. However, a small group of most active, high-$\dot{M}$ SU UMa stars, called ER UMa stars, has been recently established near the period minimum (Kato & Kunjaya, 1995; Nogami et al., 1995; Kato et al., 1999), and the evolutionary state of ER UMa stars is a serious problem (Nogami, 1998).

Var73 Dra was discovered by Antipin & Pavlenko (2002) on the Moscow archive plates. Their following CCD observations in 2001 August–October proved that this star is an SU UMa-type dwarf nova of $R = 15.7$ at the supermaximum and the recurrence cycle of the normal outburst is 7–8 days. The superhump period ($P_{\rm SH}$) was measured to be 0.0954(1) day, but the possibility of its one-day alias, 0.1053 d, could not be rejected.

Var73 Dra is identified with USNO B1.0 1546–0228545 ($B1 = 15.90, R1 = 16.09$), the proper motion of which is not listed in the catalog. The SIMBAD Astronomical Database does not give any cross-identification for this object other than the USNO entry.

We started an intensive photometric-observation campaign of Var73 Dra since 2002 October to reveal behavior of this newly discovered in-the-gap SU UMa-type dwarf nova. The results including two well-covered superoutbursts are reported in this paper.

2. Observations

The observations were carried out at ten sites with twelve sets of instruments. The log of the observations and the instruments are summarized in Table 1. Figure 1 is a finding chart where the comparison stars are marked.

All the frames obtained at Hida and Okayama, and frames at Saitama on 2002 October 14 were reduced by the aperture photometry package in IRAF[1], after de-biasing (Hida frames) or dark-subtraction (Okayama and Saitama frames), and flat-fielding. The Kyoto frames and the rest of the Saitama frames were processed by the PSF photometry package developed by one of the authors (TK). All frames obtained at the DeKalb Observatory, CBA Belgium, and CBA Concord were reduced by aperture photometry after dark subtraction and flat-fielding, using the AIP4WIN software by Berry and Burnell[2]. The Crimean images were dark subtracted, flat-fielded and analyzed with the profile/aperture photometry package developed by one of the authors (VPG).

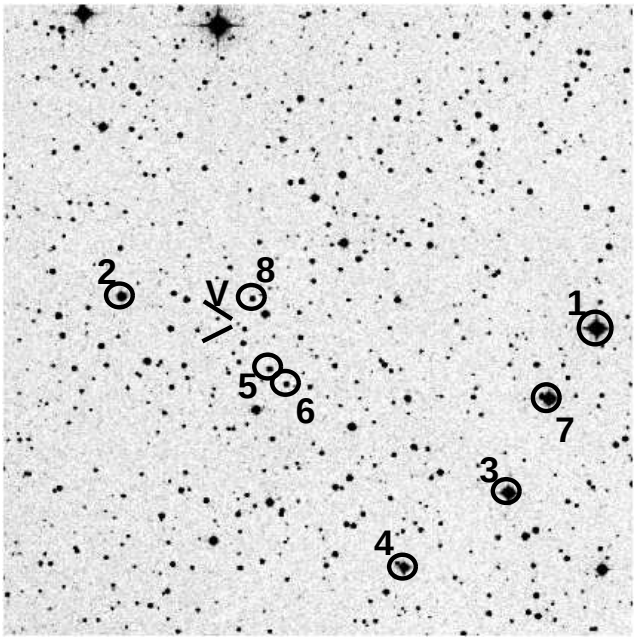

Fig. 1. Finding chart of Var73 Dra generated by the astronomical image-data server operated by National Astronomical Observatory of Japan, making use of Digital Sky Survey 2 (Region ID: XP106, Plate ID: A0LI). North is up, and East is left. The field of view is $13' \times 13'$. The numbers from 1 to 8 are given to the comparison stars in Table 1

3. Results

The long-term light curve is shown Fig. 2. During our monitoring, Var73 Dra gave rise to three superoutbursts: the first was in the rising phase on HJD 2452553, the second began on some day between HJD 2452611 and HJD 2452614 (see Table 1), the precursor of the third superoutburst was caught on HJD 2552674. This fact proves the supercycle of Var73 Dra to be ∼60 days. While two normal outbursts were caught at the start and around HJD 2452650 in the long-term light curve shown in Fig. 2, our observations reject the possibility of the recurrence cycle of the normal outburst shorter than 15 days.

[1] IRAF is distributed by the National Optical Astronomy Observatories for Research in Astronomy, Inc. under cooperative agreement with the National Science Foundation.

[2] http://www.willbell.com/aip/index.htm

Table 1. Log of observations.

Date			HJD-240000 Start–End	Exp. Time (s)	N	Comp. Star*	Relative Mean Mag.	filter	Instr.†	Superhump
2002	August	29	52516.109–52516.257	30	240	1	6.5(0.3)	no	A	
		30	52517.106–52517.206	30	170	1	8.0(0.9)	no	A	
	September	1	52519.114–52519.213	30	199	1	10.7(2.7)	no	A	
		2	52520.103–52520.177	30	105	1	10.2(2.5)	no	A	
		3	52520.104–52520.196	30	217	1	10.0(2.4)	no	A	
		4	52522.117–52522.215	30	228	1	10.5(3.1)	no	A	
		5	52523.093–52523.210	30	277	1	9.4(2.3)	no	A	
		8	52526.088–52526.208	30	280	1	9.7(2.0)	no	A	
		9	52527.091–52527.190	30	230	1	11.6(3.7)	no	A	
		10	52528.113–52528.207	30	216	1	9.6(2.1)	no	A	
		18	52536.052–52536.220	30	398	1	11.8(4.2)	no	A	
		19	52537.053–52537.135	30	195	1	10.1(2.9)	no	A	
		20	52538.086–52538.172	30	203	1	11.8(4.5)	no	A	
		21	52539.123–52539.207	30	197	1	9.2(2.0)	no	A	
		24	52542.089–52542.214	30	294	1	>8.0	no	A	
		25	52543.089–52543.128	30	308	1	11.2(3.7)	no	A	
	October	2	52550.025–52550.117	30	219	1	10.6(3.5)	no	A	
		3	52551.081–52551.127	30	106	1	6.2(1.0)	no	A	
		5	52553.023–52553.116	30	150	1	5.2(0.2)	no	A	
		9	52557.070–52557.130	30	138	1	5.2(0.2)	no	A	
		10	52557.993–52558.082	30	211	1	5.3(0.2)	no	A	○
		11	52558.993–52559.082	30	210	1	5.3(0.3)	no	A	○
		12	52559.981–52560.081	30	230	1	5.4(0.2)	no	A	○
		13	52560.674–52560.784	100	80	2	3.3(0.2)	Clear	B	○
		13	52560.917–52561.236	45	309	2	3.5(0.1)	no	C	○
		13	52560.931–52561.187	40	161	2	3.2(0.2)	no	D	
		13	52560.943–52561.238	30	314	2	3.0(0.4)	no	E	○
		13	52560.944–52561.084	60	139	2	3.0(0.1)	*B*	F	○
		13	52560.994–52561.196	30	477	1	5.9(0.3)	no	A	○
		14	52561.600–52561.762	120	107	8	1.1(0.1)	*R*	G	○
		14	52561.885–52562.187	60	329	2	3.5(0.1)	*V*	F	○
		14	52561.926–52562.223	40	173	2	3.3(0.4)	no	D	
		14	52561.946–52562.225	30	82	2	2.9(0.7)	no	E	
		14	52562.020–52562.228	55	151	2	3.7(0.2)	no	C	○
		15	52562.532–52562.696	120	71	8	1.1(0.1)	*R*	G	○
		15	52562.616–52562.722	60	145	2	3.5(0.1)	Clear	H	○
		15	52563.044–52563.230	30	436	1	6.2(0.3)	no	A	
		15	52563.129–52563.266	55	118	2	3.7(0.2)	no	C	○
		16	52563.991–52564.011	30	45	1	5.8(0.2)	no	A	
		16	52564.147–52564.266	115	82	2	3.7(0.3)	no	C	○
		17	52564.567–52564.666	150	52	8	1.3(0.2)	*R*	G	○
		17	52564.979–52565.174	30	461	1	6.4(0.5)	no	A	
		17	52565.077–52565.237	115	103	2	3.9(0.3)	no	C	
		17	52565.401–52565.426	120	14	8	16.4(0.1)‡	*R*	K	
		18	52566.202–52566.330	90	95	8	16.5(0.1)‡	*R*	K	
		18	52566.256–52566.298	70	49	2	3.7(0.1)	*R*	I	○
		20	52567.541–52567.726	150	93	8	2.4(0.2)	*R*	G	
		20	52568.236–52568.323	180	36	8	18.1(0.2)‡	*R*	K	
		21	52568.979–52569.203	30	527	1	9.7(2.4)	no	A	
		21	52569.191–52569.227	240	5	8	16.7(0.1)‡	*R*	K	
		24	52572.221–52572.242	90	16	8	16.7(0.1)‡	*R*	K	
	November	23	52602.066–52602.123	30	136	1	10.2(2.7)	no	A	
		26	52605.143–52605.150	30	16	1	>7.4	no	A	
		27	52606.088–52606.105	30	41	1	9.8(3.0)	no	A	
		28	52607.036–52607.050	30	34	1	9.4(2.3)	no	A	
	December	1	52609.967–52609.982	30	36	1	8.3(1.4)	no	A	
		2	52610.977–52610.990	30	31	1	8.9(2.1)	no	A	
		6	52614.974–52614.993	30	45	1	5.3(0.3)	no	A	
		8	52617.336–52617.447	80	97	3	4.9(0.1)	no	J	○
		9	52617.528–52617.630	150	42	5	0.4(0.1)	*R*	G	
		9	52618.173–52618.358	200	57	8	15.9(0.1)‡	*R*	K	
		9	52618.241–52618.376	80	118	4	3.8(0.1)	no	J	○

Table 1. (continued)

Date			HJD-240000 Start–End	Exp. Time (s)	N	Comp. Star*	Relative Mean Mag.	filter	Instr.†	Superhump
		10	52618.504–52618.557	150	30	6	0.0(0.1)	no	G	○
		10	52618.871–52619.126	60	284	1	5.6(0.3)	no	D	
		10	52618.881–52619.097	30	513	1	5.4(0.2)	no	A	
		10	52619.207–52619.394	80	175	7	4.8(0.1)	no	J	○
		10	52619.235–52619.357	200	35	8	15.9(0.1)‡	*R*	K	○
		11	52619.856–52619.972	60	149	1	5.6(0.3)	no	D	○
		11	52619.873–52620.099	30	507	1	5.4(0.3)	no	A	○
		11	52620.192–52620.346	200	56	8	16.0(0.1)‡	*R*	K	○
		11	52620.243–52620.418	80	157	3	4.9(0.1)	no	J	○
		12	52620.872–52621.085	60	264	1	5.6(0.3)	no	D	○
		12	52620.876–52621.099	30	505	1	5.4(0.2)	no	A	○
		12	52621.197–52621.357	200	59	8	15.9(0.1)‡	*R*	K	
		12	52621.310–52621.381	80	58	3	4.9(0.1)	no	J	○
		13	52621.882–52622.083	60	237	1	5.6(0.3)	no	D	○
		14	52622.869–52622.970	30	232	1	5.5(0.3)	no	A	○
		15	52623.919–52624.061	60	50	1	5.4(0.4)	no	D	
		15	52624.158–52624.268	120	58	8	16.1(0.2)‡	*R*	L	
		16	52625.173–52625.297	180	45	8	16.3(0.2)‡	*R*	L	
		17	52625.919–52626.051	60	162	1	6.0(0.3)	no	D	
		18	52626.142–52626.153	180	4	8	16.2(0.1)‡	*R*	L	
		23	52631.892–52632.049	30	200	1	8.3(1.5)	no	A	
		24	52632.956–52633.050	30	73	1	8.7(2.2)	no	A	
		26	52634.923–52635.043	30	107	1	10.5(1.7)	no	E	
		27	52635.933–52636.038	30	56	1	>7.5	no	E	
		30	52638.984–52639.023	30	51	1	8.6(2.3)	no	A	
2003	January	6	52646.000–52646.058	30	139	1	>7.4	no	A	
		7	52646.934–52647.055	30	130	1	>7.5	no	A	
		8	52647.933–52648.041	30	115	1	>7.5	no	A	
		11	52650.935–52651.038	30	73	1	5.6(0.4)	no	A	
		12	52651.982–52652.033	30	84	1	6.7(0.9)	no	A	
		13	52652.990–52653.042	30	65	1	7.3(1.7)	no	A	
		16	52656.023–52656.059	30	85	1	>6.4	no	A	
		17	52656.982–52657.027	30	29	1	>6.0	no	A	
		21	52660.894–52660.909	30	16	1	11.1(3.4)	no	A	
		24	52663.931–52663.946	30	1	1	–	no	A	
		28	52667.954–52663.959	30	2	1	>7.7	no	A	
	February	4	52674.892–52674.898	30	9	1	6.9(0.9)	no	A	
		5	52675.941–52675.948	30	3	1	6.1(0.9)	no	A	
		6	52676.900–52676.905	30	3	1	>8.1	no	A	
		7	52677.903–52677.908	30	6	1	7.8(1.2)	no	A	
		11	52682.326–52682.368	30	86	1	5.3(0.1)	no	A	
		12	52683.350–52683.382	30	75	1	5.3(0.2)	no	A	
		13	52684.296–52684.384	30	209	1	5.4(0.2)	no	A	
		14	52685.290–52685.383	30	216	1	5.4(0.2)	no	A	
		15	52685.554–52685.754	60	225	2	3.3(0.1)	no	J	
		17	52687.615–52687.746	80	122	2	3.3(0.2)	no	J	

*1: USNO B1.0 4241–00865–1, $B1 = 11.48, R1 = 10.21$, 2: USNO B1.0 1546–0228620, $B1 = 13.53, R1 = 12.45$,
3: USNO B1.0 4241–01053–1, $B1 = 11.63, R1 = 10.91$, 4: USNO B1.0 1545–0231804, $B1 = 13.37, R1 = 12.05$,
5: USNO B1.0 1545–0231905, $B1 = 16.72, R1 = 15.48$, 6: USNO B1.0 1545–0231894, $B1 = 17.30, R1 = 15.59$,
7: USNO B1.0 4241–01806–1, $B1 = 11.90, R1 = 11.45$, 8: USNO B1.0 1545–0228537, $B1 = 16.51, R1 = 15.59$

† A: 30-cm tel. + SBIG ST-7E (Kyoto, Japan), B: 12.5-inch tel. + SBIG ST-7E (Alberta, Canada), C: 30-cm tel. + SBIG ST-9E (Okayama, Japan), D: 25-cm tel. + Apogee AP6E (Saitama, Japan), E: 20-cm tel. + Apogee AP7p (Saitama, Japan), F: 60-cm tel. + PixCellent S/T 00-3194 (SITe 003AB) (Hida, Japan), G: 36-cm tel. + SBIG ST-10XME, (Indiana, USA), H: 44-cm tel. + Genesis 16#90 (KAF 1602e) (California, USA), I: 80-cm tel. + SBIG ST-9 (Campo Catino Observatory, Italy), J: 35-cm tel. + SBIG ST-7 (Landen, Belgium), K: 60-cm tel. + SBIG ST-7 (Crimea, Ukraine), L: 38-cm tel. + SBIG ST-7 (Crimea, Ukraine)

‡ The magnitude is adjusted to the Johnson *R* magnitude, using $R = 15.58$ of the comparison star 9 (Antipin & Pavlenko, 2002).

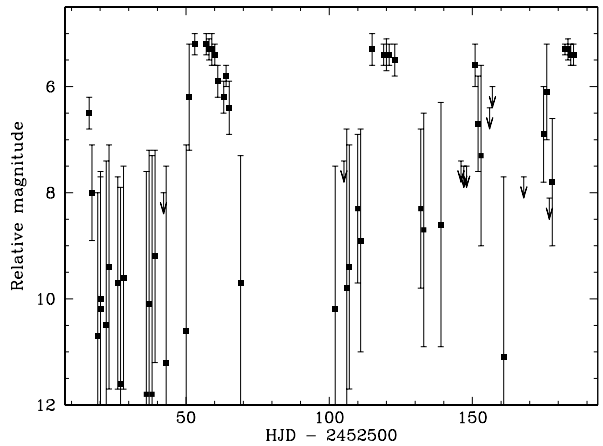

Fig. 2. Long-term light curve of Var73 Dra drawn with the Kyoto data only. The campaign was started at the decline phase of an outburst. Three superoutbursts were observed around HJD 2452560, 2452620, and 2452680. A normal outburst was recorded around HJD 2452650.

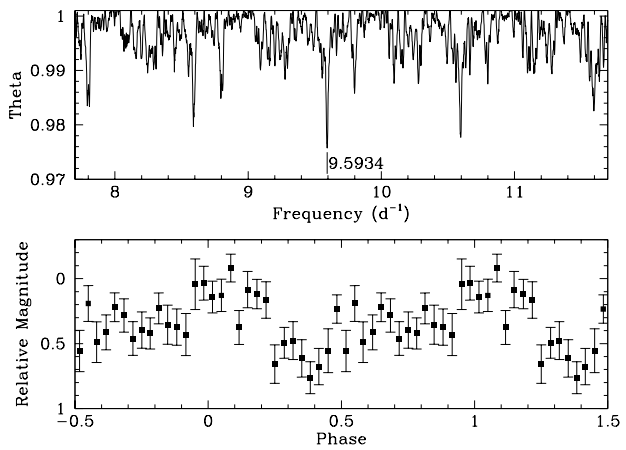

Fig. 3. a) PDM Theta diagram of a period analysis of the quiescence data between 2002 August 30 and October 3 (see text). A period of 0.10424(3) d is pointed. **b)** The quiescence light curve folded by the 0.10424-d period after subtracting the daily average magnitude from the data.

To search periodic variability in quiescence, a period analysis by the Phase Dispersion Minimization (PDM) method (Stellingwerf, 1978) was performed for the data obtained between 2002 August 30 and October 3, after excluding points over 3σ far from the daily mean magnitude and subtracting the daily mean magnitude from the daily data sets. Fig. 3 exhibits the resultant theta diagram. The sharp peak points to the period of 0.10424(3) d. The error of the period was estimated using the Lafler-Kinman class of methods, as applied by Fernie (1989). The folded light curve have a strong peak at $\phi = 0.0$ and a marginal one around $\phi \sim 0.6$.

Fig. 4 shows examples of superhumps observed during the first superoutburst. After selecting data sets with errors small enough to use for the period analysis (indicated by ○ in Table

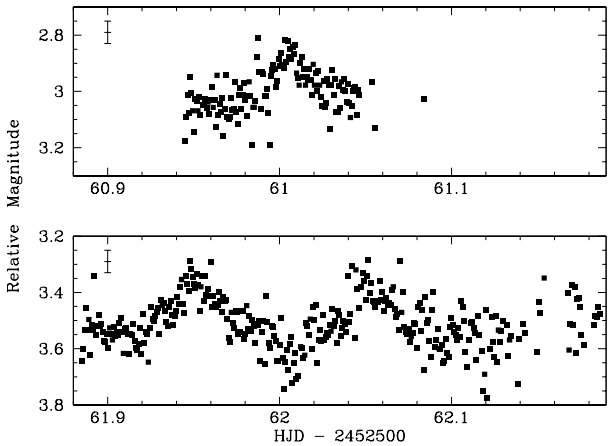

Fig. 4. Superhumps observed at the Hida observatory on 2002 October 13 (upper panel) and 14 (lower panel). The typical error bars are drawn near the upper-left corner.

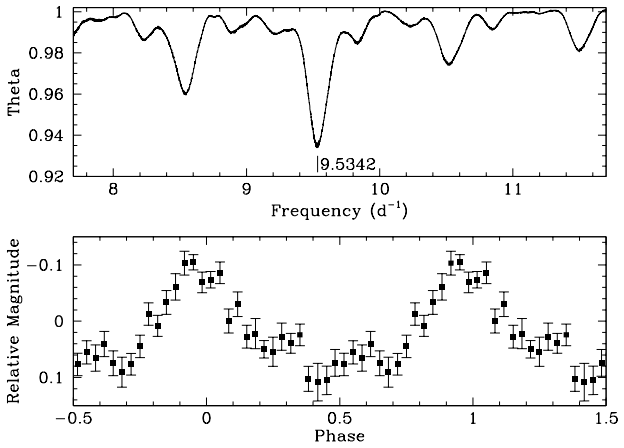

Fig. 5. a) PDM theta diagram for superhumps observed during the first superoutburst. The best estimated superhump period is 0.104885(93) d. **b)** Superhump light curve folded by the superhump period, after subtracting the mean magnitude from each data set.

1) and subtracting the mean magnitude from each data set, we applied the PDM period analysis to the processed data sets. The theta diagram and the mean superhump light curve is given in Fig. 5. The superhump period of 0.104885(93) d we obtained affirms the longer candidate proposed by Antipin & Pavlenko (2002), and assures that Var73 Dra is an in-the-gap SU UMa-type dwarf nova with the second longest $P_{\rm SH}$, next to TU Men (Stolz & Schoembs, 1984), almost equal to that of NY Ser (Nogami et al., 1998b).

We extracted the timings of the superhump maxima by fitting the average superhump light curve in Fig. 5. The results are listed in Table 2. The cycle count E was set to be 0 at the first superhump maximum measured. A linear regression and a parabolic fit to the times give the following equations:

$$HJD_{\rm max} = 61.847(1) + 0.10468(15) \times (E - 8), \quad (1)$$

Table 2. Timings of the superhump maxima during the first superoutburst.

HJD−2452500	E	O−C1*	O−C2†
61.0208(22)	0	0.0012	0.0010
61.1133(18)	1	−0.0009	−0.0011
61.6372(20)	6	−0.0004	−0.0020
62.5826(24)	15	0.0028	0.0027
62.6823(16)	16	−0.0021	0.0016

* Using Eq. (1).
† Using Eq. (2).

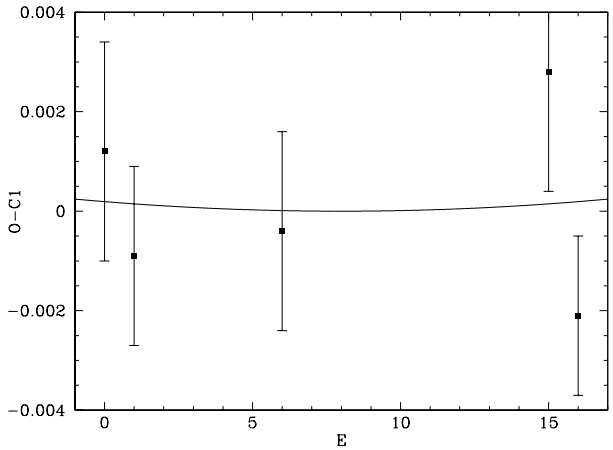

Fig. 6. $O-C$ diagram of the timings of the superhump maxima in Table 2. The calculated timings are given by Eq. (1). The parabolic curve is based on Eq. (2).

and

$$HJD_{\max} = 61.847(3) + 0.10468(18) \times (E-8) + 0.000003(56) \times (E-8)^2. \quad (2)$$

The ordinate of Fig. 3 represents the deviation of the observed timing from the expected one by Eq. (1), $O-C1$, and the curve is drawn based on Eq. (2). We could not significantly determine the change rate of the superhump period.

Fig. 7 displays the result of the PDM period analysis for the data obtained during the second superoutburst and the average superhump light curve. We used the data marked by ◯ in Table 1 also for this second $P_{\rm SH}$ analysis. The superhump period of 0.10623(16) is slightly longer than that during the first superoutburst. No apparent signal of a secondary hump around the phase of 0.5 is seen.

The timings of the superhump maxima were obtained for this superoutburst as before (Table 3). A linear regression to these timings yields the following ephemeris:

$$HJD_{\max} = 20.2513(55) + 0.10768(44) \times (E-26). \quad (3)$$

The $O-C1$ calculated using Eq. (3) is displayed in Fig. 3. The diagram clearly shows the decrease in the superhump period. Fit to a quadratic equation of the same timings gives:

$$HJD_{\max} = 20.2654(25) + 0.10756(16) \times (E-26) - 0.0000893(95) \times (E-26)^2. \quad (4)$$

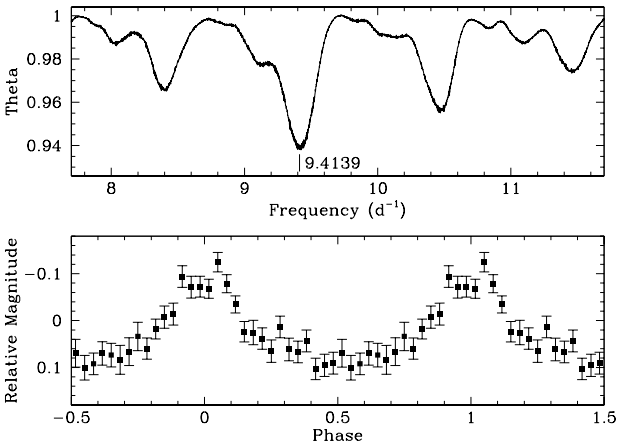

Fig. 7. a) PDM theta diagram for superhumps observed during the first superoutburst. The best estimated superhump period is 0.104885(93) d. **b)** Superhump light curve folded by the superhump period, after subtracting the mean magnitude from each data set.

Table 3. Timings of the superhump maxima during the second superoutburst.

HJD−2452600	E	O−C1*	O−C2†
17.3991(34)	0	−0.0525	−0.0094
18.5286(11)	10	0.0002	0.0070
19.2918(45)	17	0.0096	0.0017
19.2993(40)	17	0.0171	0.0092
19.9457(56)	23	0.0174	0.0038
20.0461(83)	24	0.0102	−0.0038
20.2696(26)	26	0.0183	0.0042
20.3792(39)	27	0.0202	0.0063
20.9048(51)	32	0.0074	−0.0027
21.0112(56)	33	0.0061	−0.0027
21.2189(26)	35	−0.0015	−0.0073
21.3281(38)	36	0.0000	−0.0040
21.3289(62)	36	0.0008	−0.0032
21.9520(84)	42	−0.0222	−0.0115
22.9117(56)	51	−0.0316	0.0131

* Using Eq. (3).
† Using Eq. (4).

The quadratic term means that the superhump period decreased with a rate of $P_{\rm dot} = \dot{P}_{\rm SH}/P_{\rm SH} = -1.7(2) \times 10^{-3}$, which is one order of magnitude larger than the largest values known (see Kato et al. 2003c).

4. Discussion

4.1. Two superhump periods

We obtained two superhump periods: 0.104885(93) d during the first superoutburst (hereafter $P_{\rm SH}1$), and 0.10623(16) d during the second superoutburst (hereafter $P_{\rm SH}2$). The difference

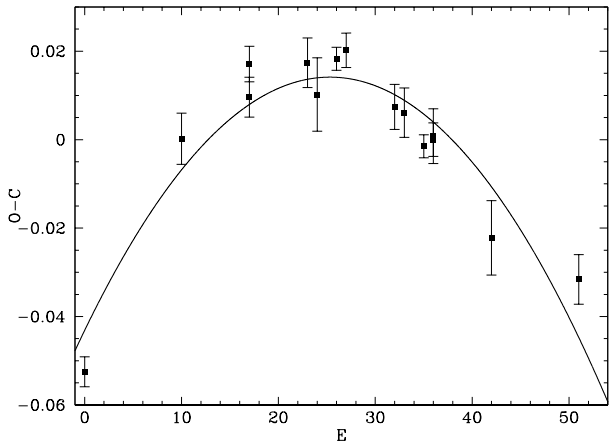

Fig. 8. $O-C$ diagram of the timings of the superhump maxima in Table 2. The calculated timings are given by Eq. (1). The parabolic curve is based on Eq. (2).

between $P_{\rm SH}1$ and $P_{\rm SH}2$ must result from difference of the observed phase in the course of the superoutburst.

The first superoutburst is estimated to have attained to its maximum brightness at HJD 2452552.0 (±1.0) from Table 1. The data used for the $P_{\rm SH}1$ analysis were therefore taken between the 6(±1)th day and the 14(±1)th day from the supermaximum. In the case of the second superoutburst, the maximum of the outburst was reached somewhen between HJD 2452611.0 and 2452615.0. Thus the data used for the $P_{\rm SH}2$ analysis were taken between the 4(±2)th day and the 9(±2)th day from the onset. Therefore the "mid" day of the observed phase during the second superoutburst (the 7(±2)th day) is earlier than that during the first superoutburst (the 10(±1) day). The extremely large change rate observed during the second superoutburst can easily yield the difference between two superhump periods.

It should be also noted that $P_{\rm SH}$ seemed to decrease with a larger rate in an earlier phase. This trend is suggested by the fact that the change rate of $P_{\rm SH}2$ was derived from the superhump-maximum times between 4(±2)th day and 10(±2)th day, in contrast to that that of $P_{\rm SH}1$ was derived from the timings of the superhump maximum between 9(±1)th day and 10(±1)th day from the supermaximum.

4.2. Orbital period

We photometrically detected coherent modulations with a period of 0.10424(3) d in quiescence. This period is slightly shorter than the superhump periods $P_{\rm SH}1$ and $P_{\rm SH}2$, and is naturally attributed to the orbital period, thus. Confirmation by spectroscopic observations is, however, desired, since our quiescence data contain large errors and the actual error of the period derived is perhaps larger than the noted one statistically calculated. The orbital period of 0.10424 d is the second longest among those of SU UMa stars with the orbital period measured, next to 0.1172 d of TU Men (Mennickent, 1995), and places Var73 Dra at the midst of the period gap.

The superhump excess ϵ (= $(P_{\rm SH}-P_{\rm orb})/P_{\rm orb}$) is 0.6% for $P_{\rm SH}1$ or 1.9% for $P_{\rm SH}2$, respectively. It is generally known that there is a robust relationship that the superhump excess smoothly increases with $P_{\rm orb}$ (see e.g. Patterson 1998). This relationship is well explainable in the disk instability model in that a large superhump excess suggests a large accretion-disk radius in a long-$P_{\rm orb}$ system with a large mass ratio ($q = M_2/M_1$). While Var73 Dra is expected to have $\epsilon \sim 5$–7% from this relation, the derived values of ϵ corresponds to those of SU UMa stars with a period about 0.06 d. This implies that Var73 Dra has a small mass ratio, although theoretical calculations on the CV evolution propose a high mass ratio for a CV in the period gap (e.g. Howell et al. 2001). Var73 Dra may be the first object which breaks the ϵ–$P_{\rm orb}$ relation[Patterson (1998) discusses this relationship after correction of $P_{\rm SH}$, taking period changes into account, to the value 4 days after superhump emergence. The same correction does not have significant effect on our results.]. This problem urges spectroscopic determination of q as well as $P_{\rm orb}$. Note that the modulations in quiescence may be attributed to permanent superhumps, as discussed later.

4.3. Derivative of the superhump period

Until mid 1990s, the superhump period was considered to monotonically decrease or at least be constant after full development (see e.g. Warner 1985; Patterson et al. 1993). This phenomenon was basically explained in the disk instability scheme by that the precession frequency of the eccentric accretion disk decreases due to shrinkage of the disk radius Osaki (1985), or propagation of the eccentric wave to the inner disk Lubow (1992). Elongation of $P_{\rm SH}$ was, however, first observed during the 1995 superoutburst of AL Com (Nogami et al., 1997). Following this discovery, similar behavior has been found in several SU UMa stars: V485 Cen (Olech, 1997), EG Cnc (Kato et al., 1997), SW UMa (Semeniuk et al., 1997; Nogami et al., 1998a), V1028 Cyg (Baba et al., 2000), WX Cet (Kato et al., 2001a), and HV Vir (Kato et al., 2001b). These stars are, however, concentrated around the period minimum in the $P_{\rm orb}$distribution, and SU UMa stars with relatively long $P_{\rm orb}$have been confirmed to show $P_{\rm SH}$ decrease with a similar rate of $P_{\rm dot} \sim -5 \times 10^{-5}$ (see Kato et al. 2003c). Very recently, Kato et al. (2003c) reported large negative derivatives of $P_{\rm SH}$ in V877 Ara ($P_{\rm dot} = -1.5(\pm0.2) \times 10^{-4}$, $P_{\rm SH} = 0.08411(2)$ d) and KK Tel ($P_{\rm dot} = -3.7(\pm0.4) \times 10^{-4}$, $P_{\rm SH} = 0.08808$ d), and pointed out a diversity of $P_{\rm dot}$ in long-period SU UMa-type dwarf novae.

We revealed that $P_{\rm dot}$ in Var73 Dra during the second superoutburst was still about one order of magnitude larger than these two records. Kato et al. (2001a) and Kato et al. (2003c) proposed a possibility that $P_{\rm dot}$is related to the mass transfer rate: SU UMa stars with larger $P_{\rm dot}$ tend to have larger mass transfer rates, and those with $P_{\rm dot}$ close to and smaller than zero have small $\dot{M}$. The quite short supercycle length of about 60 d suggests a high $\dot{M}$ in the present object (discussed later), which may support this possiblity. It should be, however, worth

noting that Kato et al. (2003a) found $P_{\rm dot} \sim 0$ in BF Ara, an SU UMa star supposed to have a rather large $\dot{M}$.

4.4. Outburst behavior

The three superoutbursts we caught suggests that Var73 Dra steadily repeats superoutbursts with a supercycle of ∼60 d. This value is shorter than the shorterst one known so far in usual SU UMa stars (89.4 d in BF Ara: Kato et al. 2003a), and close to 19–50 d of ER UMa stars.

The disk instability model predicts that the supercycle is shorter in an SU UMa-type star with a highter $\dot{M}$. Reproduction of the light curves of ER UM stars was successfully done by Osaki (1995a) by assuming a mass transfer rate about ten times higher than that in ordinary SU UMa stars (see also Osaki 1995b), although it has not still been clear why ER UMa stars have such high mass transfer rate (Nogami, 1998). Var73 Dra is expected to also have a very high mass transfer rate because of its extraordinary short supercycle (Ichikawa & Osaki, 1994). This condition may be achieved if this star is in the short, high-$\dot{M}$ phase just after getting semi-detached and starting mass transfer. This interpretation provide an explanation to the problem on the evolutionary status of this star that mass transfer is supposed to be stopped (or seriously reduced) for evolution in the period gap in the currently standard evolution theory.

This simple view, however, faces a difficulty of lack of the normal outburst in Var73 Dra. We caught two superoutbursts and two normal outbursts in the course of monitoring. The recurrence cycle of the normal outburst and the supercycle are estimated to be over 15 days and ∼60 days, respectively. In contrast, the normal-outburst recurrence cycle is expected to be ∼8 days for an SU UMa star with a supercycle of 60 days based on the model reviewed by Osaki (1996).

The normal-outburst cycle was, however, 7–8 d by Antipin & Pavlenko (2002) from their observations in 2001 August–October. The supercycle at that time was longer than at least 70 d, judging from Fig. 3 in Antipin & Pavlenko (2002). These facts clearly indicate a chage of the outburst activity between 2001 and 2002. Similar changes have been reported in recent years, such as in DI UMa (Fried et al., 1999), SU UMa (Rosenzweig et al. 2000; Kato 2002), V1113 Cyg (Kato, 2001), V503 Cyg (Kato et al., 2002), and DM Lyr (Nogami et al., 2003). Among thse stars, only DM Lyr showed an anti-correlation: the recurrence cycle of the normal outburst decreased, and the supercycle increased, while Var73 Dra showed a reverse anti-correlation: the recurrence cycle of the normal outburst increased, and the supercycle decreased. Such behavior can not be explained by variation of the mass transfer rate due to e.g. the solar-type cycle of the secondary star (e.g. Ak et al. 2001). Nogami et al. (2003) proposed for DM Lyr that a machanism to reduce the number of the normal outbursts may work when the superoutbursts more frequently occur and another mechanism to shorten the recurrence time of the normal outburst may work when the superoutburst less frequently takes place. The same idea may be applicable to Var73 Dra. Closer monitoring to avoid to miss rather faint normal outbursts (>15 mag) is needed to check variabilities of the recurrence cycles of the normal outburst and superoutburst.

4.5. Related to ER UMa stars?

Two problems regarding ER UMa stars to be solved are the extraordinary large mass transfer rates for their short orbital periods and the evolution path, as mentioned above. One of the keys to the problems is discovery of ER UMa counterparts with longer $P_{\rm orb}$.

Whether Var73 Dra is an object related to ER UMa stars is in interesting subject. While the supercycle of ∼60 d is certainly very close to those of ER UMa stars, our observations give a negative support to this question in terms of the duty cycle of the superoutburst and the recurrence cycle of the normal outburst. The duration of the supercycle of Var73 Dra is at most 15 d (Table 1), a normal one for an SU UMa system, and the duty cycle of the superoutburst in one supercycle is ∼25%, while the duty cycle is 30–50% in ER UMa stars. The normal outburst is 1 or at most a few in one supercycle, quite infrequent for an ER UMa analog.

New interpretations on how ER UMa stars most frequently give rise to superoutbursts have been recently published, which are based on the disk instability scheme, but assuming decoupling of the thermal and tidal instability (Hellier, 2001), or the effects of irradiation (Buat-Ménard & Hameury, 2002). Both models predict superhumps observed in quiescence. The modulations observed here in quiescence may be superhumps, which could give a solution to the problem that the superhump excess in Var73 Dra is too small for this long $P_{\rm orb}$. A small mass ratio is, however, a basic assumption in both models. Measurement of the orbital period and the mass ratio in this system has a significant effect also on this matter.

Kato et al. (2003b) discovered a peculiar behavior of superhumps in ER UMa which is a phase shift of 0.5 before entering the plateau phase of the superoutburst, and interpreted that the (normal) superhumps are seen at the very early phase of the superoutburst and the modulations observed during the plateau phase correspond to 'late' superhumps in SU UMa stars. To trace the superhump evolution throughout a superoutburst is important to clarify the superhumps in Var73 Dra exhibit the normal SU UMa-type behavior or the ER UMa-type one.

Acknowledgements. This research has made use of the USNOFS Image and Catalogue Archive operated by the United States Naval Observatory, Flagstaff Station (http://www.nofs.navy.mil/data/fchpix/), and the SIMBAD database, operated at CDS, Strasbourg, France (http://simbad.u-strasbg.fr/Simbad). GM acknowledges the support of Software Bisque and Santa Barbara Instrument Group. This work is partly supported by a grant-in aid (13640239) from the Japanese Ministry of Education, Culture, Sports, Science and Technology (TK), and by a Research Fellowship of the Japan Society for the Promotion of Science for Young Scientists (MU).

References

Ak, T., Ozkan, M. T., & Mattei, J. A. 2001, A&A, 369, 882
Antipin, S. V. & Pavlenko, E. P. 2002, A&A, 391, 565

Baba, H., Kato, T., Nogami, D., et al. 2000, PASJ, 52, 429
Buat-Ménard, V. & Hameury, J.-M. 2002, A&A, 386, 891
Fernie, J. D. 1989, PASP, 101, 225
Fried, R. E., Kemp, J., Patterson, J., et al. 1999, PASP, 111, 1275
Hellier, C. 2001, PASP, 113, 469
Howell, S. B., Nelson, L. A., & Rappaport, S. 2001, ApJ, 550, 897
Ichikawa, S. & Osaki, Y. 1994, in Theory of Accretion Disks-2, ed. W. J. Duschl, J. Frank, F. Meyer, E. Meyer-Hofmeister, & W. M. Tscharnuter (Dordrecht: Kluwer Academic Publishers), 169
Kato, T. 2001, Inf. Bull. Variable Stars, 5110
Kato, T. 2002, A&A, 384, 206
Kato, T., Bolt, G., Nelson, P., et al. 2003a, MNRAS, in press (astro-ph/0301565)
Kato, T., Ishioka, R., & Uemura, M. 2002, PASJ, 54, 1029
Kato, T. & Kunjaya, C. 1995, PASJ, 47, 163
Kato, T., Matsumoto, K., Nogami, D., Morikawa, K., & Kiyota, S. 2001a, PASJ, 53, 893
Kato, T., Nogami, D., Baba, H., et al. 1999, in Disk Instabilities in Close Binary Systems, ed. S. Mineshige & J. C. Wheeler (Tokyo: Universal Academy Press), 45
Kato, T., Nogami, D., & Masuda, S. 2003b, PASJ, in press (astro-ph/0211520)
Kato, T., Nogami, D., Matsumoto, K., & Baba, H. 1997, Tech. rep.
Kato, T., Santallo, S., Bolt, G., et al. 2003c, MNRAS, 339, 861
Kato, T., Sekine, Y., & Hirata, R. 2001b, PASJ, 53, 1191
King, A. R. 1988, QJRAS, 29, 1
Kolb, U. & Baraffe, I. 1999, MNRAS, 309, 1034
Lubow, S. H. 1992, ApJ, 401, 317
Mennickent, R. E. 1995, A&A, 294, 126
Nogami, D. 1998, in ASP Conf. Ser. 137, Wild Stars in the Old West, ed. S. Howell, E. Kuulkers, & C. Woodward (San Francisco: ASP), 495
Nogami, D., Baba, H., Kato, T., & Novák, R. 1998a, PASJ, 50, 297
Nogami, D., Baba, H., Matsumoto, K., & Kato, T. 2003, PASJ, in press (astro-ph/0301036)
Nogami, D., Kato, T., Baba, H., & Masuda, S. 1998b, PASJ, 50, L1
Nogami, D., Kato, T., Baba, H., et al. 1997, ApJ, 490, 840
Nogami, D., Kato, T., Masuda, S., et al. 1995, PASJ, 47, 897
Olech, A. 1997, Acta Astron., 47, 281
Osaki, Y. 1985, A&A, 144, 369
Osaki, Y. 1989, PASJ, 41, 1005
Osaki, Y. 1995a, PASJ, 47, L11
Osaki, Y. 1995b, PASJ, 47, L25
Osaki, Y. 1996, PASP, 108, 39
Paczyński, B. 1971, ARA&A, 9, 183
Patterson, J. 1998, PASP, 110, 1132
Patterson, J., Bond, H. E., Grauer, A. D., Shafter, A. W., & Mattei, J. A. 1993, PASP, 105, 69
Robinson, E. L. 1983, in Cataclysmic Variables and Related Objects, ed. M. Livio & G. Shaviv (D. Reidel Publishing Company, Dordrecht), 1
Rosenzweig, P., Mattei, J., Kafka, S., Turner, G. W., & Honeycutt, R. K. 2000, PASP, 112, 632
Semeniuk, I., Olech, A., Kwast, T., & Nalezyty, M. 1997, Acta Astron., 47, 201
Stellingwerf, R. F. 1978, ApJ, 224, 953
Stolz, B. & Schoembs, R. 1984, A&A, 132, 187
Warner, B. 1985, in Interacting Binaries, ed. P. P. Eggelton & J. E. Pringle (Dordrecht: D. Reidel Publishing Company), 367
Warner, B. 1995, Cataclysmic Variable Stars (Cambridge: Cambridge University Press)
Webbink, R. F. & Wickramasinghe, D. T. 2002, MNRAS, 335, 1
Whitehurst, R. 1988, MNRAS, 232, 35